Final Report - Approved for Public Release

SBIR Phase I Topic: 13-1-022

Title: "Radar Derived Bathymetry."

Contractor: Areté Associates

Contract Period: Aug 1, 2013 - Feb 25, 2014

Submitted by:
Steven Anderson
Areté Associates
1550 Crystal Dr., Suite 703
Arlington, VA 22202
703-413-0290 x4055

This material is based upon work supported by the National Oceanic and Atmospheric Administration (NOAA) under contract number WC-133R-13-CN-0084. Any opinions, findings, conclusions or recommendations expressed in this publication are those of the author(s) and do not necessarily reflect the views of the NOAA.

Project Summary

NOAA can reduce costs and improve efficiency by remotely monitoring harbors, navigation channels and coastlines for bathymetric changes. This will aid NOAA in its mission to maintain waterways and assure maritime safety.

The long-term program goal is to develop and transition the capability to remotely measure shallow water bathymetry suitable for navigation use in real-time using marine X-band radars. This will require producing robust algorithms and a software system suitable to use in safe navigation that incorporates permanent shore-based radar installations and ship mounted radars to provide real-time survey and "look ahead" capability. This software would be transitioned to NOAA, port and harbor authorities, USCG and the private sector.

This report describes the R&D effort under Phase I. This effort included:

- Collecting x-band radar data from a shore based operationally relevant location.
- Benchmarking the derived bathymetry against NOAA supplied ground truth (measured bathymetry) and documenting accuracy, range, minimum and maximum depths, and spatial resolution.
- Exploring next generation algorithms for derived bathymetry retrievals leveraging recent advances in Fourier modeling techniques and computational speed.

We successfully demonstrated radar bathymetry with an existing algorithm showing an accuracy of approximately 1 m, with an objective of 25 cm, over depths ranging from 4 to 20 meters. We benchmarked the results and lessons learned against feasibility metrics and conclude that an operational bathymetric radar capability is within reach using existing technology. Our proposed implementation plan leverages existing radar infrastructure with cloud based computing to archive, process and disseminate derived bathymetry.

This Phase I study addresses the feasibility of a shore based bathymetric radar system. However, all the lessons learned are directly applicable to a ship based radar system. In this application, a ship would use its x-band radar to survey the surrounding bathymetry in real-time to improve navigation safety.

The success of Phase I will hopefully lead to prototyping and demonstrating a real-time, shore based radar bathymetric capability. These are the first steps toward reaching NOAA's long term goal of an operational remote bathymetric measurement system suitable for both land and ship based radar systems.

Report Outline

1) Research Objectives

NOAA can reduce costs and improve efficiency by remotely monitoring harbors, navigation channels and coastlines for bathymetric changes. This will aid NOAA in its mission to maintain waterways and assure maritime safety.

The long-term goal is to develop and transition the capability to remotely measure shallow water bathymetry suitable for navigation use in real-time using marine X-band radars. This will require producing robust algorithms and a software system suitable to use in safe navigation that incorporates permanent radar installations in ports and harbors, and ship mounted radars to provide real-time survey and “look ahead” capability. This software would be transitioned to NOAA, port and harbor authorities, USCG and the private sector.

The overall SBIR program "13-1-022" goals are to:

- Produce robust versions of the algorithms, reduced to software that can be used by NOAA, port and harbor authorities, and other agencies to measure water depth in real time so as to be able to provide that information to ships for safe navigation.
- Develop a complete commercial system incorporating the software which is suitable for permanent deployment in ports and harbors to monitor water depth.
- Generalize the algorithms and software so they can be included in any marine X-band radar, including those already aboard ship, to give them real time water depth measurement of their own with look-ahead capability.

The purpose of this NOAA SBIR Phase I program is to conduct research and development which will allow the Government to determine the technical merit and feasibility of using a new radar derived bathymetry capability. This will help the government decide if further investment will produce a cost effective and practical solution to measure water depths in real time with a precision, accuracy, and resolution suitable for navigation use.

The NOAA and the International Hydrographic Organization (IHO) have not yet defined specific requirements and standards for radar bathymetry. It is recognized that derived bathymetry may never reach the resolution and accuracy of accepted (bathymetric sonar and LIDAR) technologies. The expectation is that radar bathymetry will not meet existing IHO standards. However, it will complement existing technologies by providing persistence; continually monitoring for bathymetric changes from sediment transport, change in water levels and emerging hazards to navigation. In addition, radar imagery can provide other information important for navigation including surface currents and location of breaking waves and other hazards to navigation. Dierssen and Theberge (2014) review the range of accepted and emerging technologies for measuring bathymetry. Their analysis yields an illustrative synopsis of how radar bathymetry fits in with spatial resolution and accuracy of traditional techniques (See Figure 1).

So what represents feasibility for bathymetric radar? Discussions with NOAA helped shape possible system performance and development requirements that would be required for practical application.

We put forward the following feasibility metrics for this SBIR. For radar bathymetry to be feasible, we should demonstrate, or show clear path towards, a system and algorithms that:

- Uses commercial off the shelf (COTS) radar and computer hardware. No new hardware development required and the software is adaptable to a range of commercial systems.
- Can readily undergo software refactoring for real-time processing of bathymetry retrievals on COTS computer.
- meets these performance metrics as compared to IHO standard bathymetry.
    - Range: ~3000 m
    - Spatial resolution: ~100 m
    - Temporal resolution: 30-60 minutes

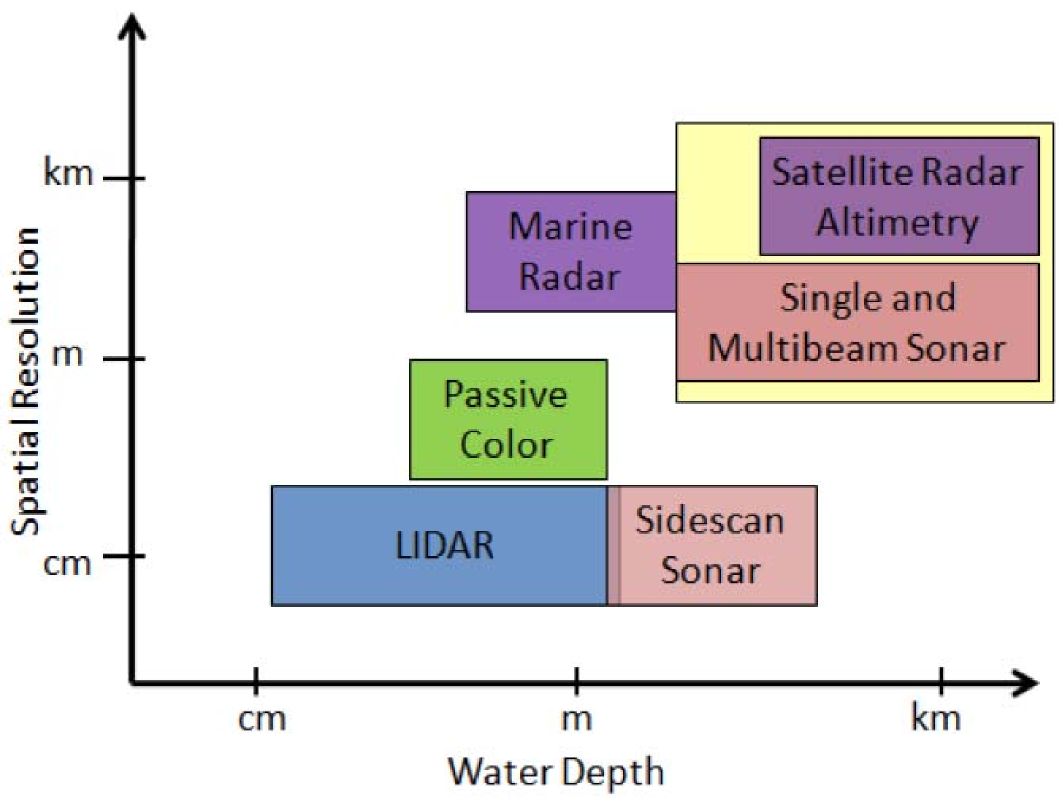

Figure 1. Schematic showing the applicability of different techniques for estimating bathymetry in terms of spatial resolution of measurement and the range in water depths that can be sampled. (From Dierssen and Theberge, 2014).

  - Accuracy: 25 cm
  - Depth range: 3 m (outside surf zone) to 20 m
- Will operate under a range of wind-wave-swell conditions at operational locations.

This report describes the R&D effort under Phase I. This effort included:

- Deploying an x-band marine radar and collecting data in a region that is operationally relevant.
- Benchmarking the derived bathymetry using an existing algorithm (Three-Dimensional Power Spectral Density - 3-D PSD) against NOAA supplied ground truth (measured bathymetry) and documenting accuracy, range, minimum and maximum depths, and spatial resolution.
- Exploring next generation algorithms for derived bathymetry retrievals leveraging recent advances in Fourier modeling techniques and computational speed.

The success of Phase I will hopefully lead to prototyping and demonstrating a real-time, shore based radar bathymetric capability. These are the first steps toward reaching NOAA's long term goal of an operational remote bathymetric measurement system suitable for both land and ship based radar systems.

2) <u>Approach</u>

a) <u>Review of Approach and Existing Commercial Systems</u>

Shoaling gravity waves were first used to derive water depths during WW II to assist planning for amphibious landings. Thus, the wave-based bathymetry retrieval approach is over 60 years old. The method was first disclosed in Williams (1947) and Seiwell (1947). The technology was crude at the time, but imaging from aircraft provided data adequate for making the appropriate manual calculations to assist the planning for amphibious assaults. This has been further developed and improved off and on over intervening years. Young et al (1985) first used a standard marine navigation radar to retrieve surface water currents, also indicating how water depths could be retrieved as part of the algorithm. The basis for this technique is the *dispersion relation* for linear gravity waves on water with uniform or slowly varying current and water depth (see Equation 1).

Since the Young et al (1985) paper, there have been over 50 papers published in technical society journals and conference proceedings on the use of this principle for retrieving water depths. A review of all the algorithms and their advantages and disadvantages for radar bathymetry application is beyond the scope of this report. However, we direct the reader to the following wave dispersion based bathymetry retrieval algorithms in the recent literature: the 3-D Power Spectral Density (3-D PSD; Piotrowski and Dugan, 2002), C-Bathy (Holman et al, 2013), DiSC (Senet et al, 2008) and normalized scalar product (NSP; Ludeno et al, 2014). There are similarities between these algorithms and they all have significant limitations for the proposed application. A primary issue is that these algorithms rely on direct use of the dispersion relation for slowly varying bathymetry, and, on Fourier analysis and processing of the 3-D power spectrum (as described in the next Section).

There are several technology issues that must be addressed before radar derived bathymetry can seriously be considered for operational utility. One issue is a lack of error budgets and ground truthing to determine its accuracy as a function of numerous environmental and radar system parameters. A second limitation is the lack of an appropriate algorithm that can provide spatial resolution that is demonstrably superior to that having been reported in the literature to date. Both of these issues are within range of viable solutions.

Two companies already market radar systems with a bathymetry measurement capability:

> *OceanWaveS GmbH* (http://www.oceanwaves.de/) sells the Wave and Surface Current Monitoring System WaMoS® II that has been developed for real time measurement of directional ocean wave spectra. OceanWaveS has demonstrated that WaMoS can provide currents and water depths.
>
> *Nortek* sells the SeaDarQ radar system (http://www.seadarq.com/) for use on vessels or on land to detect and track oil spills. This system also provides current and bathymetry. The system specification for bathymetry is -- Depth Range: up to 30 m; Accuracy: ±0.5 m.

These systems use proprietary algorithms but the evidence suggests that they are based on linear wave dispersion and would have similar limitations as the algorithms noted above. The stated system accuracies of these commercial systems have not been independently validated through peer review or by NOAA. To the defense of these radar providers, bathymetry retrieval is not a primary capability for their principal markets and so it has likely not yet received significant R&D investment.

Our feasibility study approach includes collecting data from a COTS marine radar system while NOAA Coast Survey independently collects ground truth bathymetry. This approach assures the ground truth meets NOAA standards. We also gathered wind, wave, current and water level data from nearby NOAA operational systems so the results can be considered in context of environmental conditions at the time of collection.

We implemented the 3-D PSD as a low risk approach to demonstrate feasibility. There were two reasons we chose to use the 3-D PSD: (1) Alternative algorithms (such as DiSC and NSP) have demonstrated bias, while the 3-D PSD has been shown to be bias free for cases with good wave signatures and larger spatial resolutions. (2) Our group developed the 3-D PSD algorithm and has great experience implementing it on a range of passive imaging system for the US Navy. However, this is the first time we implemented it for a marine X-band radar.

We also believe the science and technology is now right for a next generation bathymetry algorithm which does not rely on linear wave-dispersion over flat or slowly varying bathymetry. This will allow for the highest possible spatial resolution for bathymetry.

b) Description of 3-D PSD algorithm

Equation 1. Linear Wave Dispersion

$$\omega = (gk \tanh(kh))^{1/2} + \boldsymbol{U}*\boldsymbol{k}$$

where

ω is the wave frequency
g the acceleration of gravity
h the water depth
k the scalar wavenumber
k the vector wavenumber
U the vector current.

Note: the ***U*k*** vector product term is the Doppler shift in frequency due to the current and it can be retrieved in parallel with the water depth.

The 3-D spectral approach is summarized here. The image data are assembled as a temporal stack of geometric 'images'. Each image is the equivalent of the range-azimuth maps of radar cross section as typically seen on PPI displays. The radar cross section is the power returned from a typical navigation radar system with maritime horizontal polarization transmit / horizontal polarization receive (HH) antenna. An important assumption is then made; that there is a linear modulation transfer function (MTF) between the waves and these radar returns. Then, the 'wave' data are assembled into a grid made up of x-y-t data 'cubes' and these are pre-processed and Fourier transformed into 3-D frequency-wavenumber (ω-***k***) spectra, one for each data cube. The dispersion relation (actually a 2-D surface in 3-D ω-***k*** space) is fit to the 3-D spectrum, with the depth, *h,* as the free parameter of the fit. This value is reported out as the water depth for that data cube, and it is posted at the center location of the spatial grid box. Finally, the assembly of the results for all the data cubes is the resulting water depth field for the stage of the tide at the time the imagery was collected. Using separately recorded tidal data, these water depths are transformed into tidal datum referenced bathymetry data.

A fundamental limitation of the 3-D spectral approach is the assumption that the underlying bathymetry in each data cube is constant and the wave field homogeneous and stationary. The low frequency, long waves are most sensitive to the depth and, therefore, of the most interest. The stationarity assumption is satisfied as long as the temporal dwell (duration) of the sequence of images is long enough. Resolving the lowest frequency waves (swell) in the wave field can be an issue as there are fewer of them for a given dwell. If the temporal dwell is too short, there will be too few long waves and the spectrum will not be stable. This is not typically a problem with radars on the shore since the dwell can be unlimited, assuring an adequate estimate of all the wave frequencies in the spectrum. A further issue is the effective spatial resolution, limited by the required spatial size of the data cubes. In order to obtain good estimates of the swell wavelength (the *k* in Equation 1), the data cubes must contain many waves, and our experience is that 5 or more waves are necessary to achieve this. Thus, the data cubes being so large, the results provide poor density of postings.

3) Data Collection

a) Instrumentation

For the data collection, we used an Areté owned Furuno X-Band FAR-2127-BB Series radar with a transmit power of 25 kW and the capability of resolving 10.5 meters in range. The antenna is an 8 foot model (XN-24AF) with a beamwidth of 0.95° horizontal and 20° vertical and a rotation rate of 42 rpm. The radar can record returns out to 10 km ranges at a resolution of 10.5 m. The radar samples at 3000 pulses per second at 42 RPM yielding a pulse every ~0.1° in azimuth. The wide antenna and fast rotation rate make this commercial radar suited to image ocean waves. (We noted that this model radar is the same as one of the radars used operationally at the Cape Henry Pilot Tower.)

We used a Curtiss Wright Osiris PMC/PCI Radar Interface card that allows a great deal of flexibility in how the radar data are collected, stored and even processed in real time. Data was recorded to internal hard drives and then copied onto external USB disks for near real-time data assurance and post processing. Recording was configured to digitize the radar with a resolution of 3m in range and 0.1 degree in azimuth.

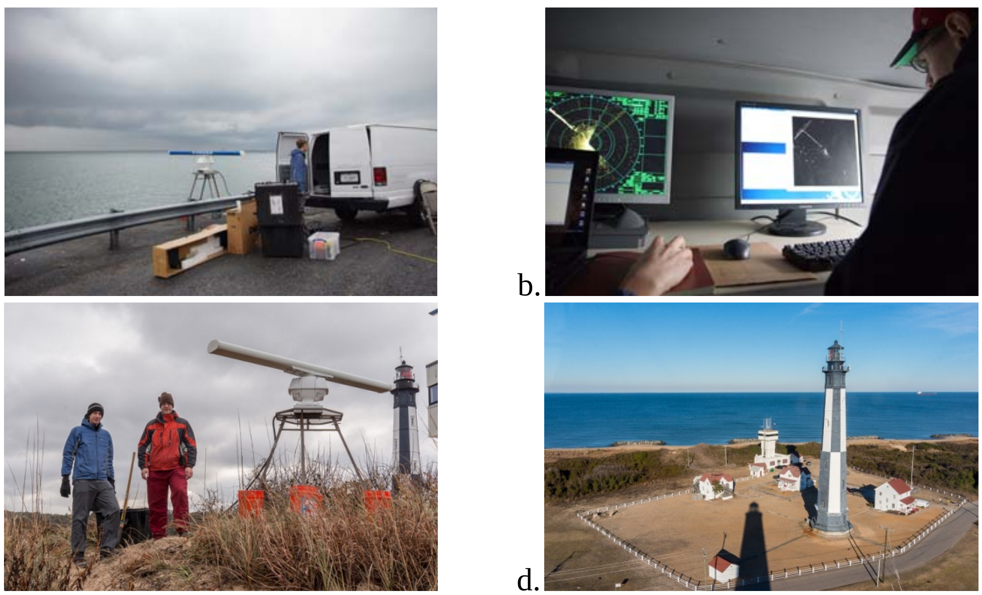

a. b. c. d.

Figure 3. Pictures from field collections. (a) Radar at CBBT Island 2. (b) Collection systems in back of van. (c) Radar at Cape Henry Lighthouse. (d) Cape Henry lighthouse and pilot tower.

We used the top section of a hunting stand for mounting the antenna. This placed the antenna approximately 3 meters above the ground. The legs of the stand were each set in five gallon buckets that were then filed with sand thus providing anchors for stability. The radar control, display and acquisition system was set up in the back of a cargo van. This allowed us to quickly (< 2 hours) set up and break down (<30 minutes) the radar. Installation pictures are in Figure 3.

Table 1. Site locations and times of collection.

		(local)
CBBT Island #2 36.980806° N 76.106205° W	October 22, 2013	1400 - 1700
	October 23, 2013	0930 - 1615
Cape Henry Lighthouse 36.927248° N 76.006529° W	December 10, 2013	1615 - 1645
	December 11, 2013	0845 - 1700
	December 12, 2013	0830 - 1130

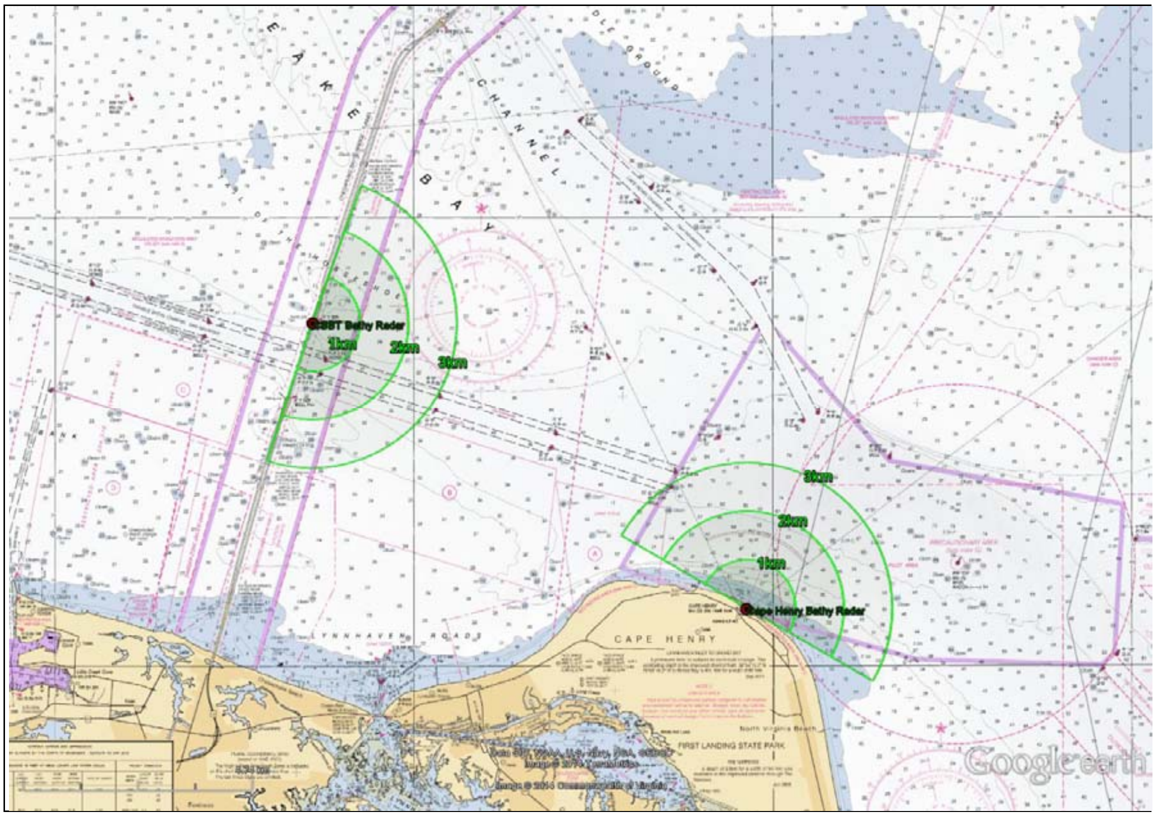

Figure 4. Radar collection locations at Chesapeake Bay Bridge Tunnel (CBBT) Island 2 and Cape Henry Lighthouse. The green rings indicate ranges of 1 km, 2 km and 3 km.

b) Site Descriptions

The radar was deployed once to the Chesapeake Bay Bridge Tunnel (CBBT) and once to Cape Henry. The locations and collection times are noted in Table 1 and Figure 4.

i) CBBT

The deployment was located at Island Two. This is on the north side of the main navigation channel. The channel has charted depths in excess of 15 meters and shoals approaching 8 meters directly east of the radar (see Figure 4). The radar was set up on the southeast corner of the island in the parking area. The antenna was approximately 8 meters above the water. The collection region was focused towards the east and south and the radar was configured to blank transmissions to the northwest quadrant in the direction of the maintenance building. Power was obtained by running a long extension from the second floor of the maintenance building to the van. Set up, operation and break down was relatively straightforward at this site.

ii) Cape Henry

We deployed the radar on top of the dunes in front of the Pilot's Tower. This required some leg work and lifting to manually move the radar from the parking lot, through the brush and up the dunes. Our antenna cable was not long enough to reach from the dune into the Pilot's Tower. We instead positioned the van between the tower and the dune. We worked the cable down through the brush to the van. We ran a long extension cord from the second floor to the van for power. We estimated the antennae height at 12 m above the water. The location provided an unobstructed view for 180° over the water. Water depths ranged from zero (beach) to 25 m at a range of 3 km.

c) Environmental Conditions

Environmental data were obtained from NOAA buoy 44064 "First Landing" that is located north of the navigation channel at the mouth of Chesapeake Bay. This is the closest location with current, wind and wave information and we found to be representative of the conditions we observed by eye at CBBT and Cape Henry. Water level data was obtained from the tide gage located at Island One (NOAA Station ID 8638863.) Data was downloaded from the NOAA website after the radar collections and plotted in Figures 5, 6 and 7.

The conditions during the CBBT collections were dominated by a northwest wind with wind speeds ranging from 4 to 11 m/s and wave heights between 0.3 and 0.7 m. Wind waves were always clearly visible by eye and in the radar display. No swell was observable at the time of collection. The longest wave period we observed by eye was ~5 seconds. There were periods of rain during the collection period. On October 23, Buoy 44064 reported currents of ~1 m/s to the northwest at the start of collections, going slack at mid-day and then 0.7 m/s to the southeast. Water levels were rising at start, peaked at near noon and then dropped through the afternoon, with levels ranging from 0.5 to 1.1 m. We observed persistent traffic in the shipping channel.

The set up at Cape Henry occurred as a significant storm system exited the region. Winds were 10 m/s out of the north with wave heights near 1 m during installation on December 10. We managed to collect some radar before dark that had strong wave signatures. The next morning (December 11) the winds and dropped to 2-3 m/s and stayed low all day. The wave imaging by radar requires some capillary waves generated from wind to roughen the surface. Unfortunately, the very calm condition and glassy surface were less than ideal for wave imaging. On the morning of December 12, the strong north winds had returned and reported wave heights were 0.7 m. We observed persistent traffic in the shipping channel.

The water levels shown in the Figure 7 are from the NOAA Station ID 8638863 at CBBT Island One. Jack Riley (NOAA) reported to us that the Cape Henry tides lead Island One by 12 minutes and have a multiplier of 1.25 relative to mean lower low water (MLLW). Only the raw Island One data are shown in the figure, but these factors were applied when the bathymetry ground truth was compared to the bathymetric radar.

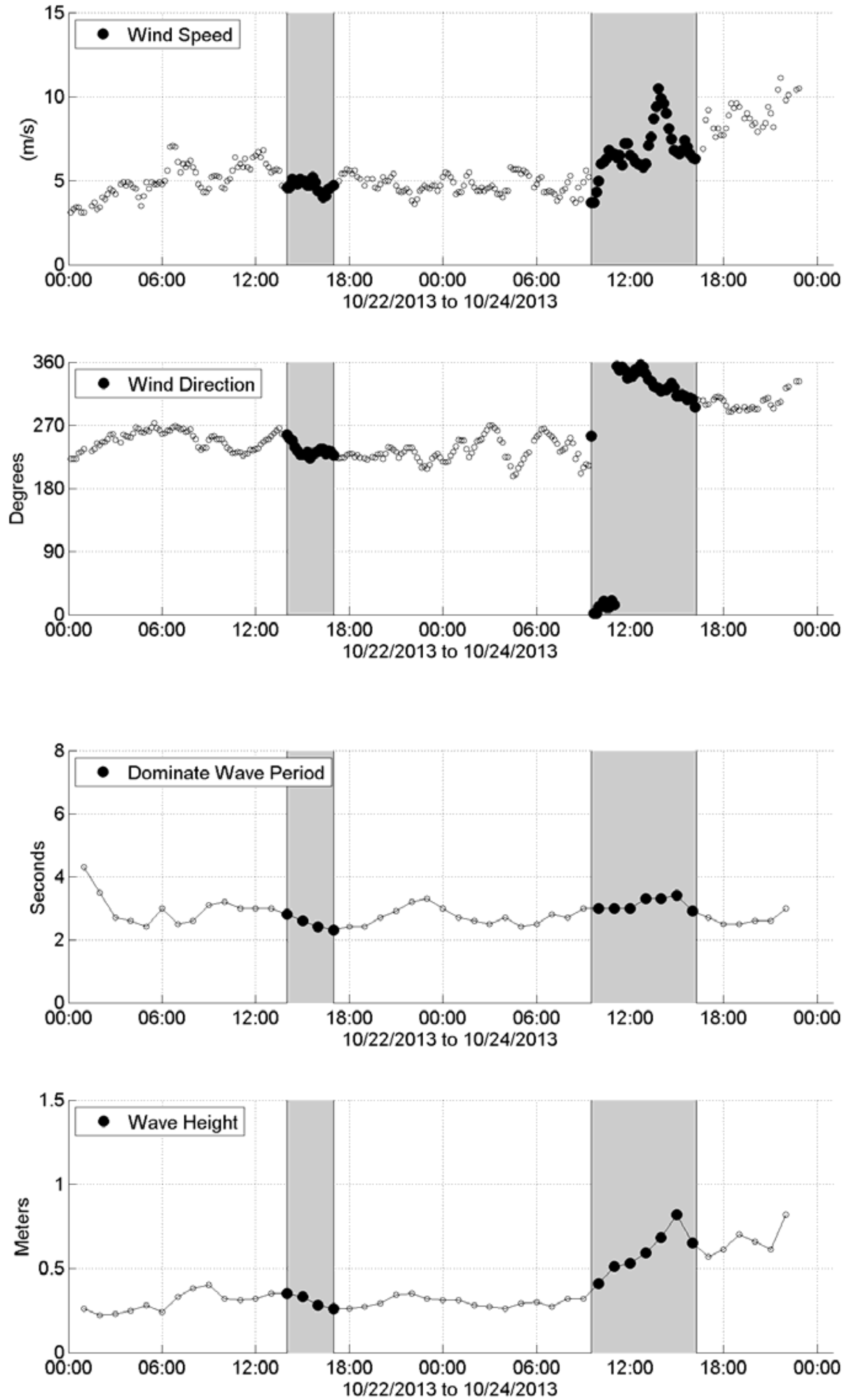

Figure 5. Wind and wave data during CBBT collections. The data was obtained from NOAA buoy 44064 located east of the radar. The grey areas indicate the time of collections.

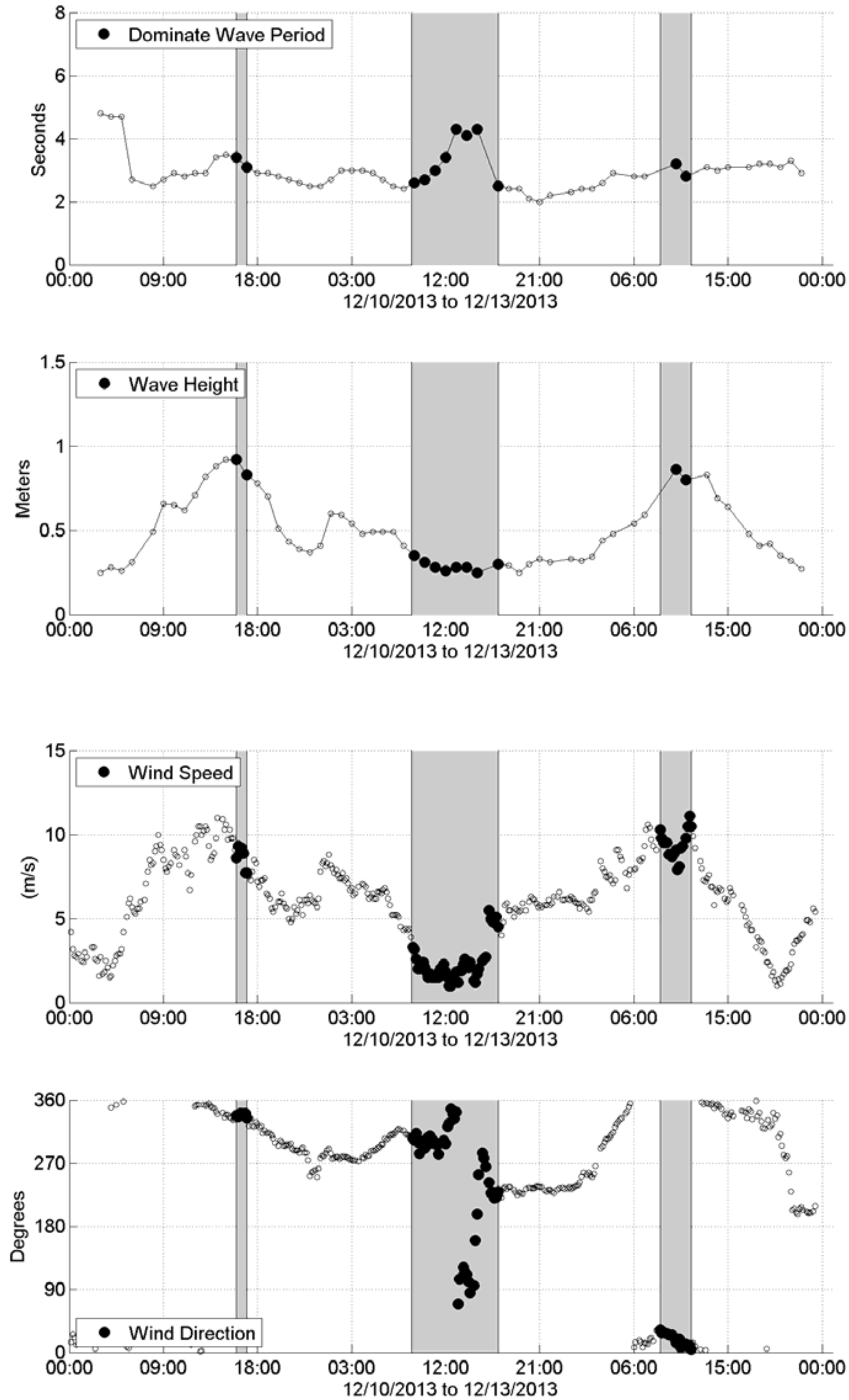

Figure 6. Wind and wave data during Cape Henry collections. The data was obtained from NOAA buoy 44064 located east of the radar. The grey areas indicate the time of collections.

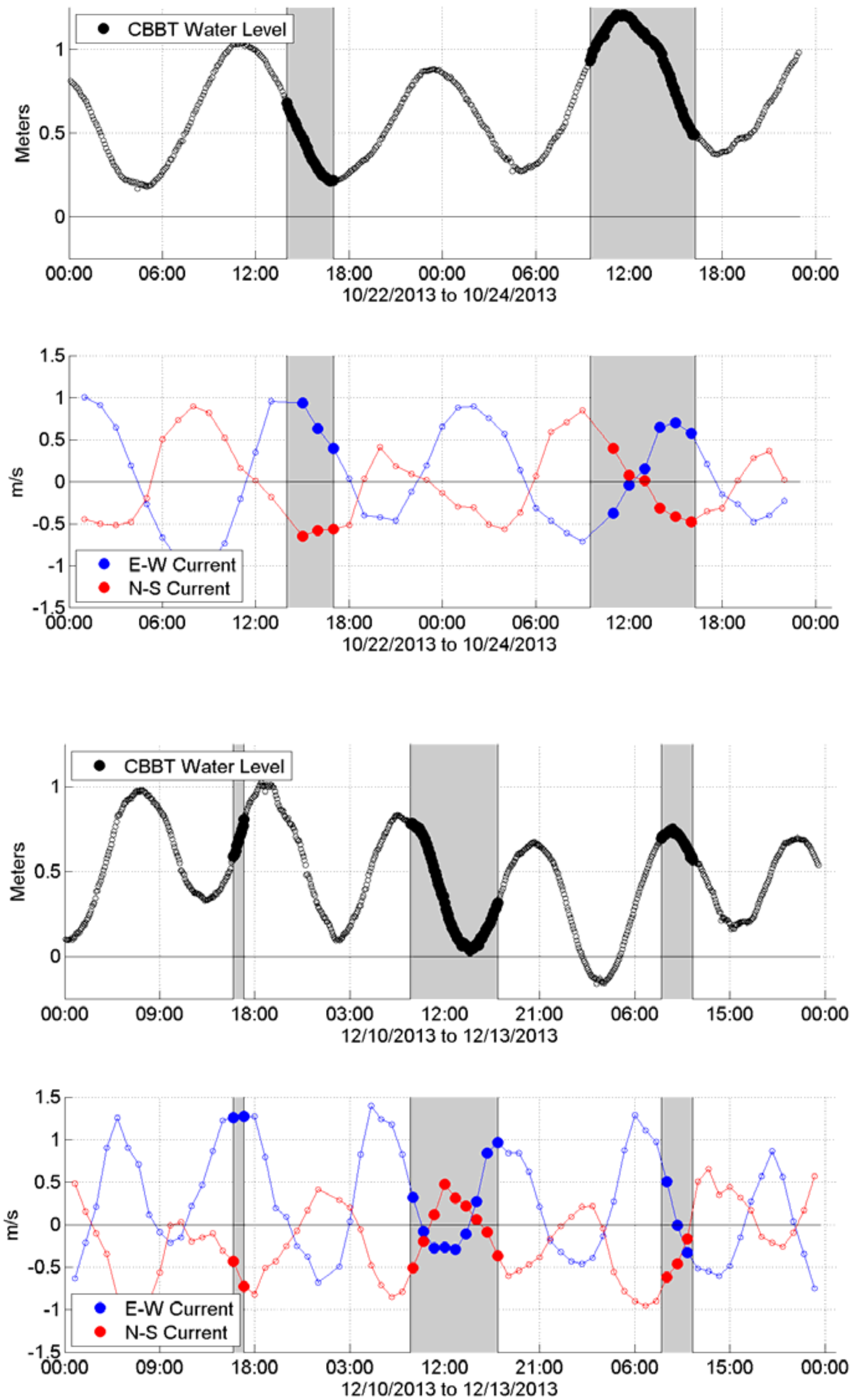

Figure 7. Water level and currents during CBBT and Cape Henry collections. The current data was obtained from NOAA buoy 44064 located east of the radar and water level is from the tide gage located at Island One (Station ID 8638863). The grey areas indicate the time of collections.

d) Description of Radar Pre-Processing

After the field collection, the data were pre-processed prior to algorithmic processing for depth retrievals. Pre-processing included:

- Assuring data integrity and time stamps and identifying data gaps.
- Mapping data to a rectilinear grid at 10 m resolution in geographic coordinates.

Examples of the raw imagery are shown in Figure 8 and Figure 9.

The following steps were not implemented but would likely further improve the bathymetry retrievals.

- Data normalization to remove variations in transmit power.
- Registration of mapped data using fixed objects in field of view as fiducials.
- Identification of boats in field of view

There is clear variation in power in the raw images which would cause some noise. There is also azimuthal jitter. We estimated this at about 0.3 degrees root mean square. We did not implement any corrections for these issues because of the limited resources available under this Phase I study. However, the image processing to improve the images is understood and straightforward. These steps would be implemented in Phase II and the operational system to provide optimal signal to noise ratios for wave imaging and bathymetry retrievals.

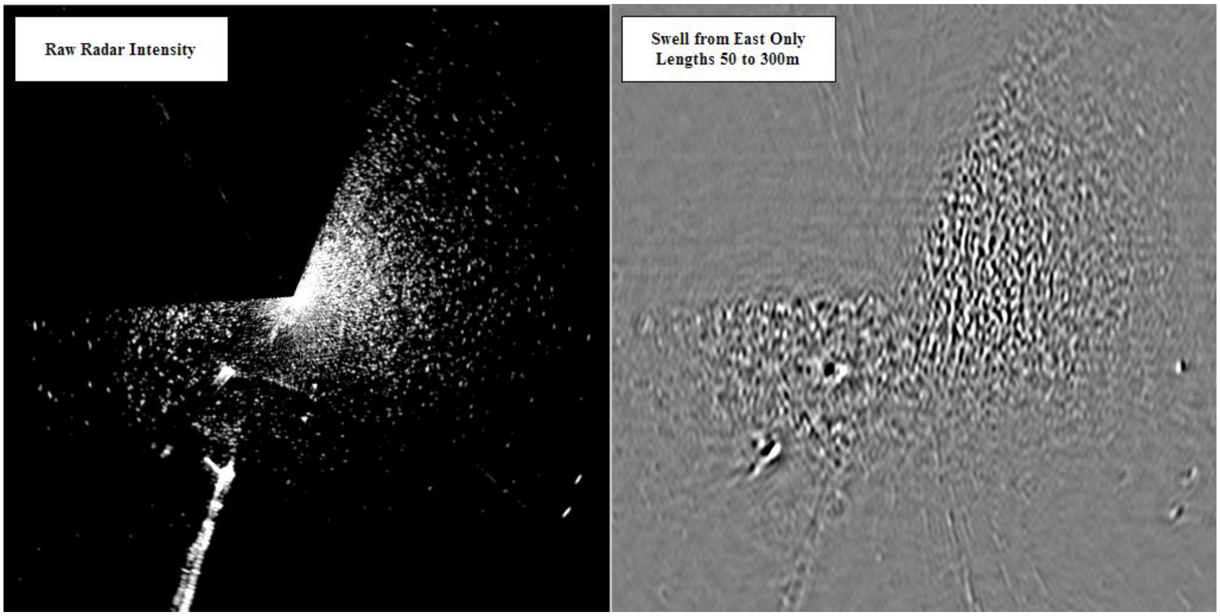

Figure 8. Example radar image from CBBT. The left panel is a single raw radar image collected at CBBT on October 23. The right panel shows the data filtered to reveal only the ocean swell propagating from the east.

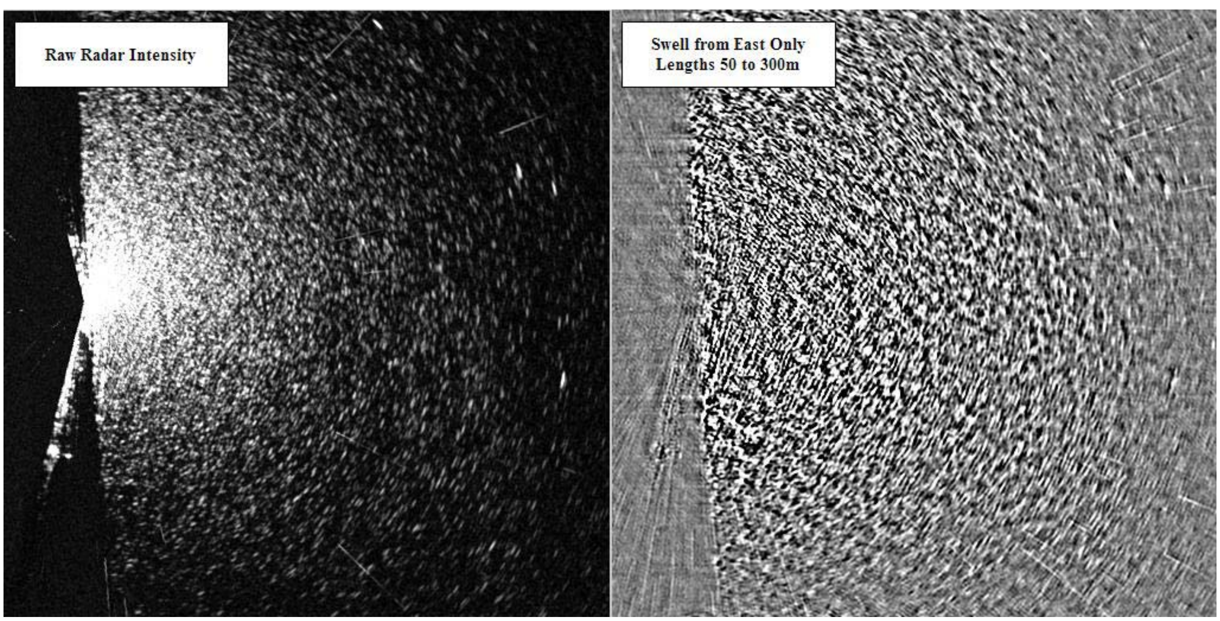

Figure 9. Example radar image from Cape Henry. The left panel is a single raw radar image collected at Cape Henry on December 10. The right panel shows the data filtered to reveal only the ocean swell propagating from the east.

e) Bathymetric Ground Truth Collections

NOAA Coast Survey conducted a bathymetric survey at both CBBT and Cape Henry in November 2013. This survey was Bay Hydro II's Bathy-Radar Project D00187. NOAA provided historical as well as the recent Bay Hydro II's sounding data. NOAA noted that their November 2013 sounding were consistent with the historical data they provided us. For best ground truth coverage, we used all historical and Bay Hydro II recent data as ground truth. The soundings were provided in MLLW coordinates and we adjusted them based on Island One water level observations and with model corrections for Cape Henry as provided by NOAA. (See Figures 10 and 11)

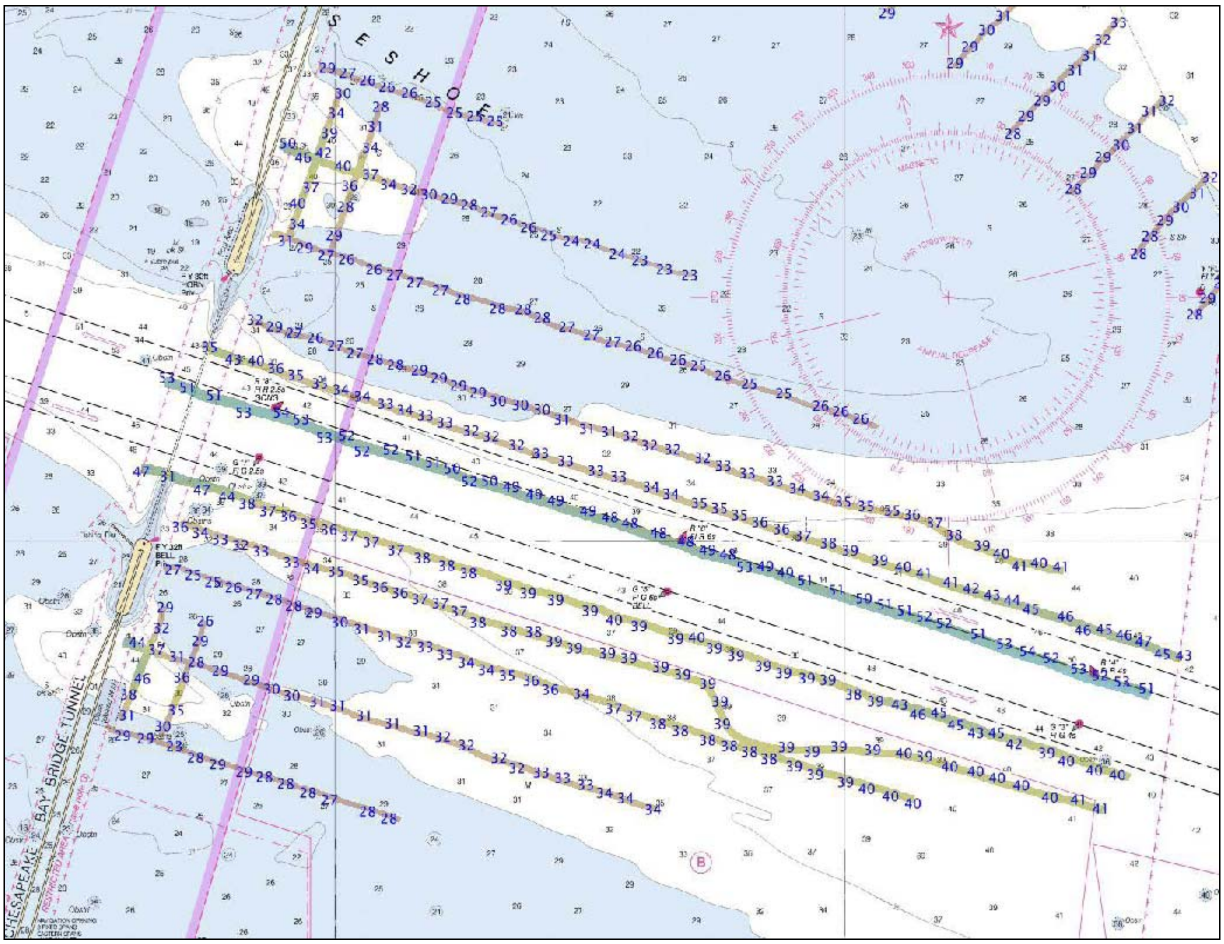

Figure 10. NOAA Bay Hydro II's Bathy-Radar Project D00187. These charts were provided by NOAA Coast Survey and indicates bathymetric data collections at CBBT that occurred in November 2013.

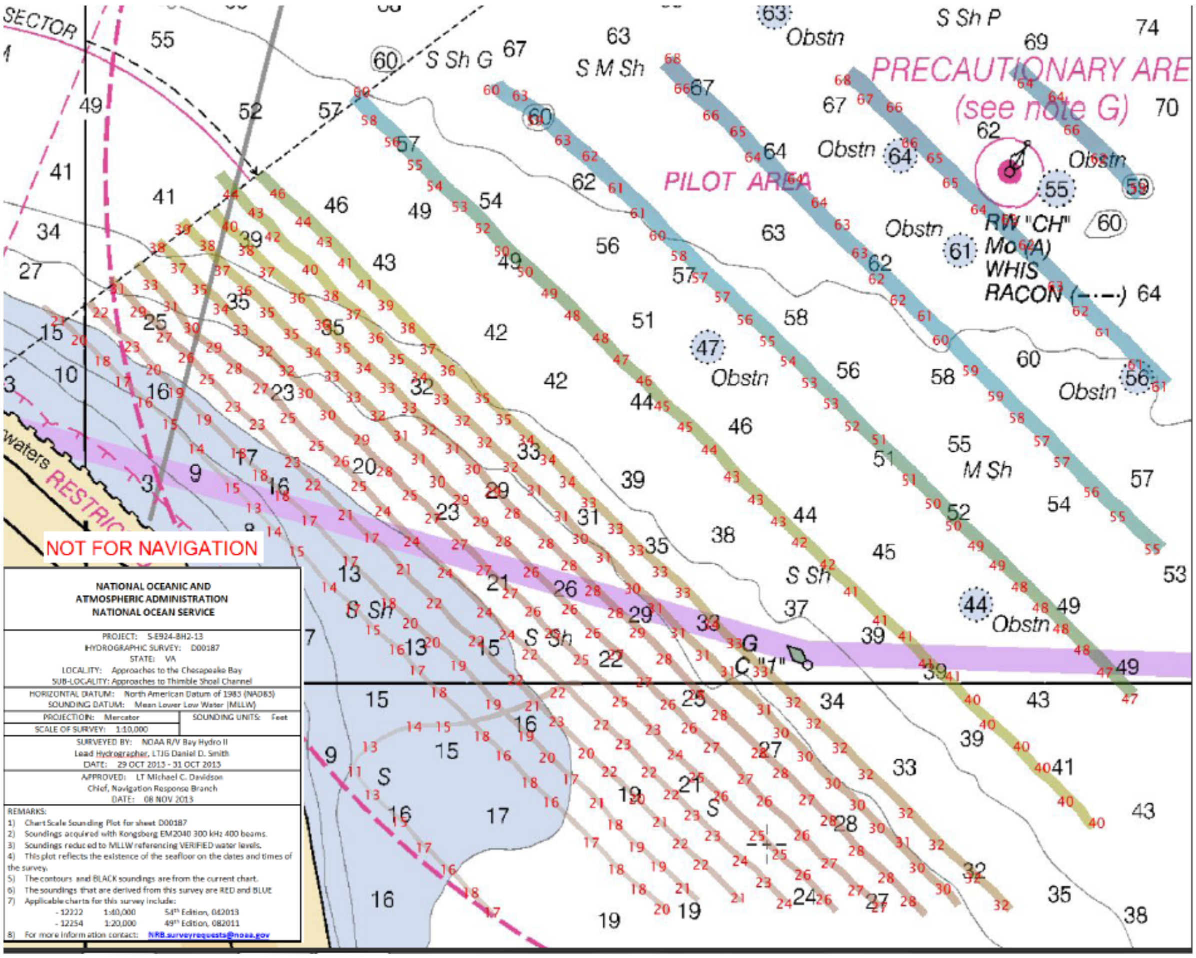

Figure 11. NOAA Bay Hydro II's Bathy-Radar Project D00187. These charts were provided by NOAA Coast Survey and indicates bathymetric data collections at Cape Henry that occurred in November 2013.

4) Results

a) CBBT

The CBBT showcases an example of how radar bathymetry can provide time varying water depths that are consistent with the observed tide.

The CBBT radar data from October 23, 2013 was characterized by a clear wind-wave signal generated by the local winds out of the northwest. These waves were visible on the raw radar display. However, no swell (period >8 seconds) is visible in the raw imagery nor by eye looking out from Island Two. These longer waves are critical to bathymetric extractions, especially as the water gets deeper. Fortunately, there was a detectable swell from the east in the data after further signal processing.

Figure 12 is a chart of the CBBT region that shows the location of two analysis "tiles": 1344m x 1344m and 672m x 672m. The larger tile allows for better wavenumber resolution and analysis of longer waves. Figure 13 shows a 3-D PSD from the larger tile. This is an ensemble PSD of six – five minute segments of data. Visualizing the structure of a 3-D PSD is best done by looking at slices. The first slice is a frequency-wavenumber slice in the east-west direction which is aligned with the swell from the east. The solid white line shows linear wave dispersion (Equation 1) with infinite depth and null current. The orange colored regions shows the increased energy (variance) which is a signature of waves coming from the east with periods of 5 sec (0.20 Hz) to 14 sec (0.07 Hz) and corresponding wavelengths of 40 m (0.025 cpm) to 150 m (0.007 cpm). The dashed line shows the dispersion relation with the depth of 10.5 m which bisects the area of elevated energy. The second slice is at a constant frequency of 0.08 Hz. There is an area of orange (indicating higher variance) near 0.01 cpm again showing this swell energy coming from the east.

We made three minor modifications to the 3-D PSD depth retrieval algorithm (Piotrowski and Dugan 2002) for processing the radar data. Piotrowski and Dugan (2002) developed their algorithm for airborne passive time-series imagery which has higher signal to noise ratios (SNR) than the radar data but only has limited dwell. We first enabled ensembling (averaging) of six PSD's, each calculated from consecutive 5 minute~~s~~ segments. Thus each radar bathymetry retrieval is from 30 minutes total dwell of radar data. This significantly improved the SNR of the swell in the radar data. Next, we decreased the threshold SNR for including wavenumber-frequency pairs in the dispersion curve fit. Lastly, we reduced the number of wavenumber-frequency pairs required for a depth retrieval.

The weak swell signature is only apparent in the area to the east of Island Two. No swell is observed in PSDs calculated over the channel to the south or further east or west. However, the swell signature was persistent in the tiles shown in Figure 12 throughout the day on October 23 (though the signal strength varied through the day). So we processed and present currents every half hour from this region.

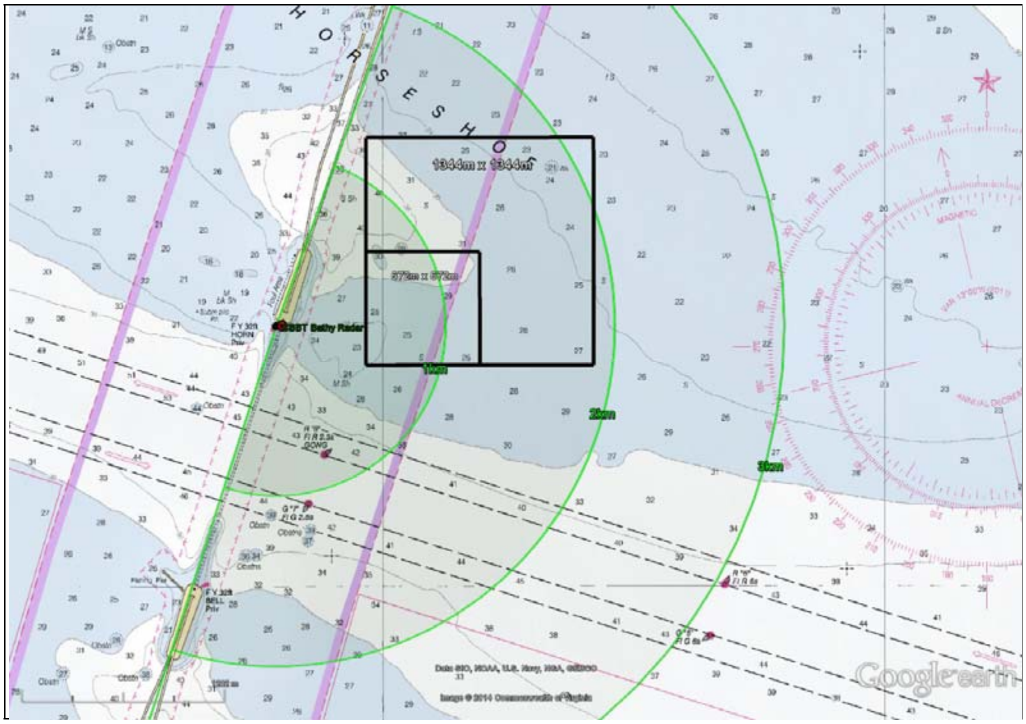

Figure 12. CBBT Bathy Radar Chart. This is NOAA Chart #12254 with the CBBT Island 2 collection location and range rings. The boxes indicate the location of the 1344m x 1344m and 672m x 672m tiles used in the depth retrieval analysis.

Piotrowski and Dugan (2002) presented results in a littoral region near a beach. Prevailing currents in these types of locations are constrained by bathymetry and typically run parallel to the beach and isobaths. The swell is mostly perpendicular to the beach. Thus, there is very little Doppler shifting of these wave and currents can be ignored for these bathymetry retrievals.

At the CBBT site, however, we found that the tidal currents had a strong east-west component and the Doppler shifting of the waves from the east would lead to 1-2 m errors in bathymetry if currents are ignored. Therefore, we first estimated the current (Figure 14) by fitting the dispersion surface to the PSD assuming a nominal depth of 10 m for the region. The derived currents for six hour period are shown in Figure 14. The currents were low in the morning, then a north-westward flow developed mid-day which reversed to a north-eastward flow in the afternoon. We do not have any current ground truth at this site, however, the east-west reversal is consistent with NOAA buoy 44064 located east of the site (Figure 6).

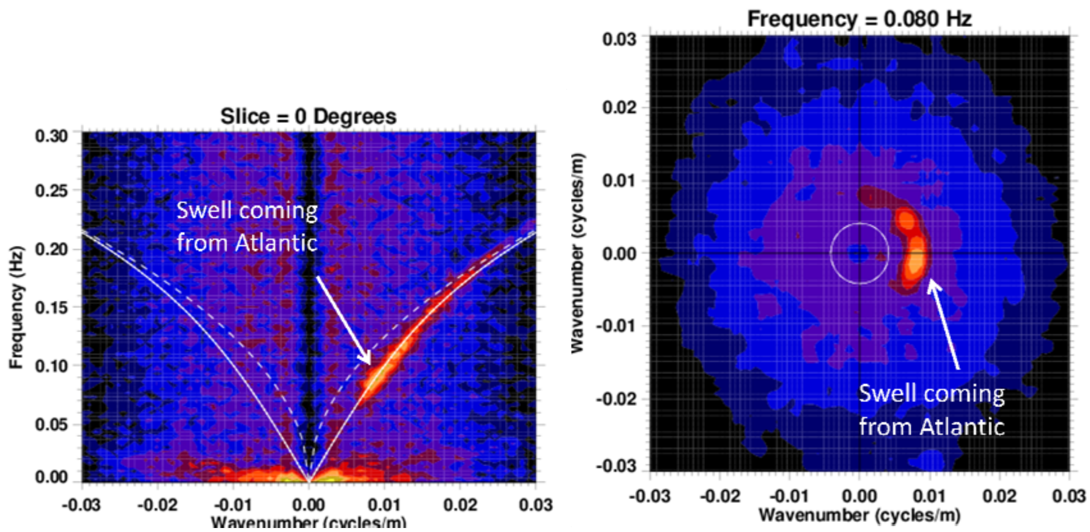

Figure 13. PSD slices of ensemble averaged 3-D PSD and Current Retrievals. The PSD are calculated from 6 ensembles, 5 minutes dwell each for a total of 30 minutes dwell total. The dashed line indicates deep water dispersion and the solid line indicates the dispersion after the depth is fit. Note: f-k slice is not in current direction, but in direction of strongest swell (due east).

Table 2. CBBT site Bathymetric Radar Performance. Truth is average of all soundings in the patch adjusted for time varying water levels observed at Island One. Also see Figure 14.

672 m x 672 m tile:

RMS = 0.37 m
Bias = -0.12 m [fit – truth]

1344 m x 1344 m tile:

RMS = 0.51 m
Bias = -0.28 m [fit – truth]

We used these currents then to derive the bathymetry every 30 minutes shown in Figure 14. These are from the 678m x 678m tile. The truth (red dots) is derived by taking an average of all NOAA provided soundings (historical and recent) within the tile and then adding observed water levels from Island One. The short dashed line indicates the minimum and maximum sound depth in the tile and the long dashed lines indicate bounds of 50% of the soundings. The retrieved bathymetry (blue) dots are presented every 30 minutes. Note: for an operational algorithm, we would implement and iterative the process to solve for the current vector and bathymetry that best fits to the observed dispersion relation in the 3-D PSD.

The statistical results for 1344m x 1344m and 672m x 672m tiles are shown in Table 2. We were unsuccessful at retrieving currents and bathymetry for 336 m x 336 m tiles. Examination of the 3-D PSD does show a dispersion relation. However, there are only a handful of wavenumber-frequency pairs since the swell signature is very weak, and the waves are narrow banded. This did not yield enough pairs for a least squares fit. We suspect that further refinement of the algorithm would yield a meaningful result at smaller scale for this particular case.

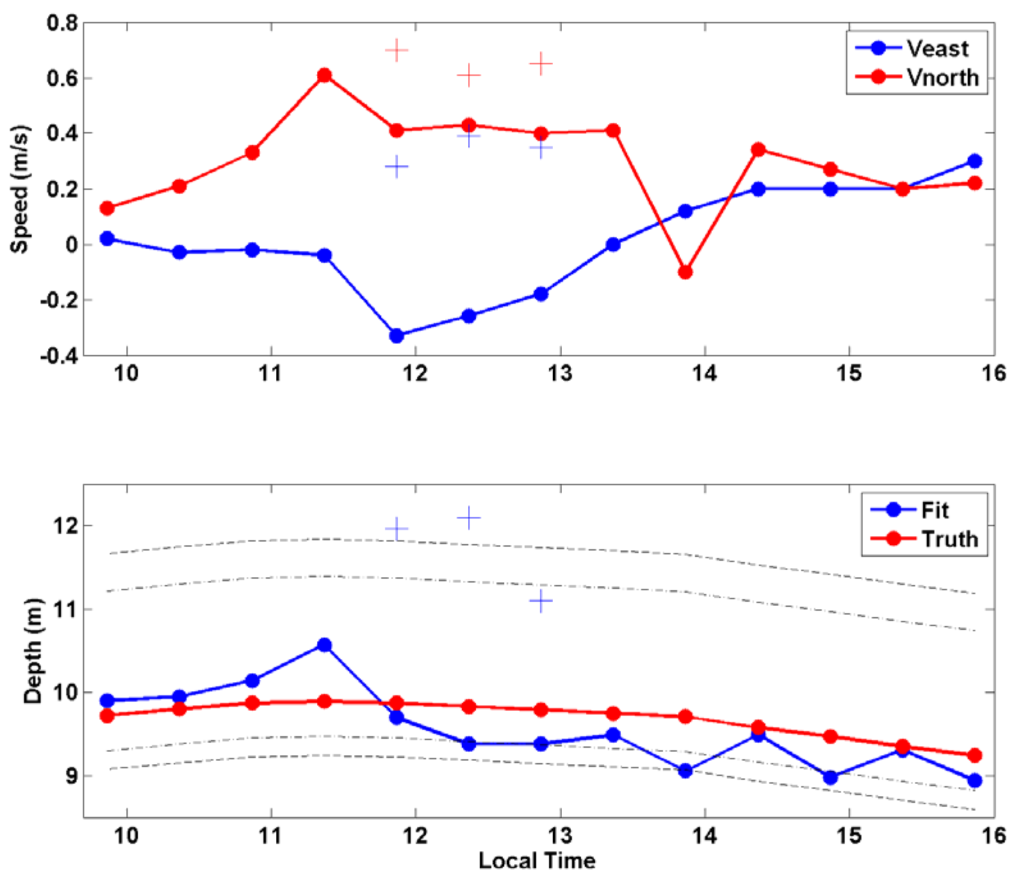

Figure 14. CBBT Current and Depth Retrievals. These are retrievals from the 672 m x 672 m tile shown in Figure 13. The top figure is the current vector components retrieved from the radar each half hour. In the bottom figure, the red dots are truth: the average of all soundings in the patch adjusted for time varying water levels observed at Island One. The blue dots are the retrieved depth every half hour. The short dashed line indicates the minimum and maximum sound depth in the tile and the long dashed lines indicate bounds of 50% of the soundings.

b) Cape Henry

The Cape Henry data is an example of how radar bathymetry provides spatial coverage of bathymetry in a range of depths from the 4 meters (surf zone) to 20 meters out to a range of 2 km.

The Cape Henry data from December 10, 2013 was characterized by a strong wind (8 m/s) from the north and wave heights of 0.9 m. The radar was set up as a storm system moved out of the region and we collected 40 minutes of radar data before sunset. Waves were clearly visible in the radar data and swell (period >8 seconds) could be observed breaking on the beach.

An example 3-D PSD is shown in Figure 15. The PSD shows swell (~12 second period) arriving from the east and wind waves coming from the north. There is sufficient signal to noise (SNR) in the wave energy for depth retrievals. There is also extra variance of low frequency and wavenumber in the same direction as the wind waves. The source of this variance is likely associated with the wave breaking as the white caps move slower than the linear waves. This variance is well below the dispersion curve and does not interfere with the depth retrievals in this case.

The depth retrievals were obtained on 336 m and 672 m tiles with 50% overlap. The ground truth was computed by averaging both historical and the recent Bay Hydro II's Bathy-Radar sounding in each tile. The soundings have been adjusted to the observed water levels at Island Two with a scale factor of 1.25 relative to MLLW.

We found excellent agreement between observed and radar retrievals for 336 m tiles for water depths of 4 to 10 meters (Figure 16). The bias is 0.1 m and the root mean difference 1.2 m. However, retrievals in water deeper than 10 m have a clear bias as can be seen in Figure 16 and no depth retrievals were possible at depths beyond 12 m.

We suspect this bias is a result of longer wavelengths encountered in the deeper water. To explore the source of this deep bias beyond 10 m, we recalculated retrievals with 672 m tiles (see Figure 17). The 672 m tiles yield successful retrievals from 8 m to 22 m and the bias, observed beyond 10 m with 336 m tiles, disappears. For the 672 m tiles, the bias is -0.3 m and the root mean difference 1.7 m. (Note that the shallower waters (<8 m) are not represented because the tiles are too big to fit close to the beach.)

This result is consistent with the fundamental limitation of the 3-D spectral algorithm. In 10 m water depth, the observed swell period of 12.5 seconds and has a wavelength of 120 m. This is only about 3 times the 336 m tile size and the wavenumber information is no longer adequately resolved. However, the larger tiles do accurately resolve the wavelengths and yield the correct depths. This is a clear example of the limitation of the 3-D PSD algorithm. It would be straightforward to implement enlarging the tile size based on the water depth into the algorithm.

The radar bathymetry retrievals are overlaid with the nautical chart in Figure 18. This shows that retrievals were obtained out to a range of ~2 km with the 336 m tiles.

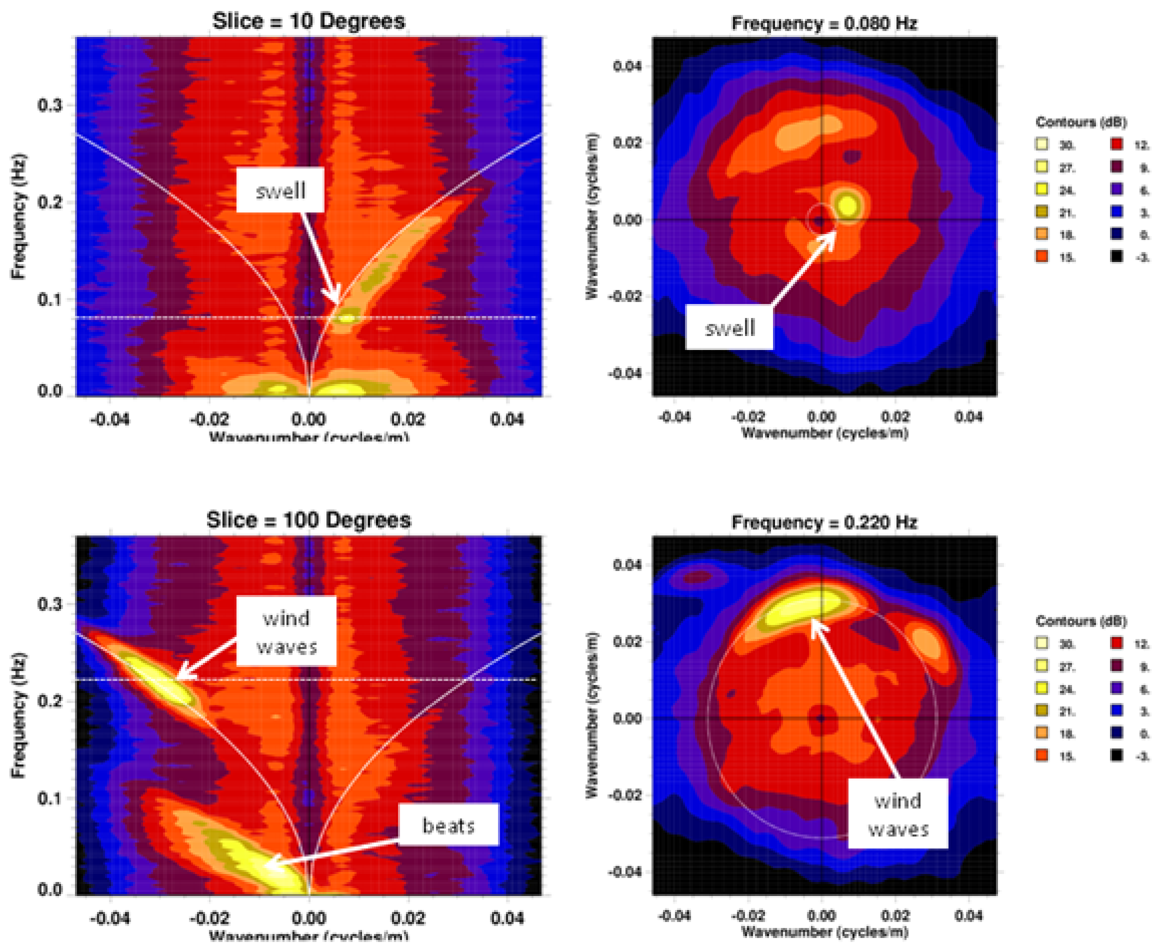

Figure 15. Cape Henry 3-D Power Spectral Density. The PSD is calculated from 6 ensembles, 5 minutes dwell each, for a total of 30 minutes dwell total. The solid line indicates deep water dispersion. The figures on the right are wavenumber slices in the direction of the swell (top) and the wind-waves (bottom). On the right are frequency slices at 0.08 Hz (12.5 seconds) and 0.22 Hz (4.5 seconds) showing the swell coming in from the east (top) and wind waves from the north (bottom). Note: on the f-k slice for the wind waves (bottom left) there is a lot of energy at low frequency in the direction of the wind waves. This extra energy (labeled "beat") is off the dispersion curve and likely from the strong wave breaking. It does not interfere with the depth retrievals in this case.

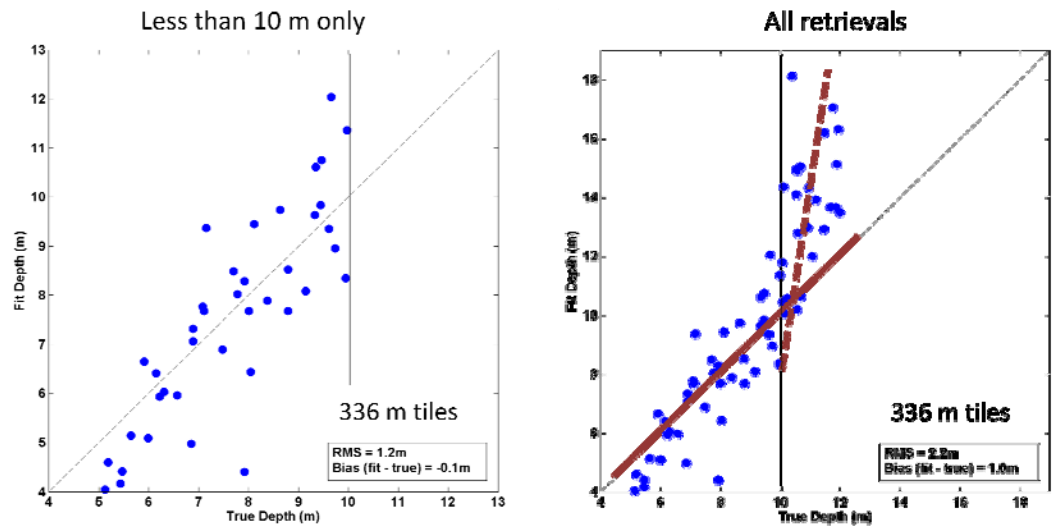

Figure 16. Cape Henry Bathy Radar compared to Ground Truth. The depth retrievals from the 336m x 336m tiles with 50% overlap are shown. The panel on the left shows all the points where the observed depth was less than 10 m and the panel on the right shows all points where there was a successful retrieval.

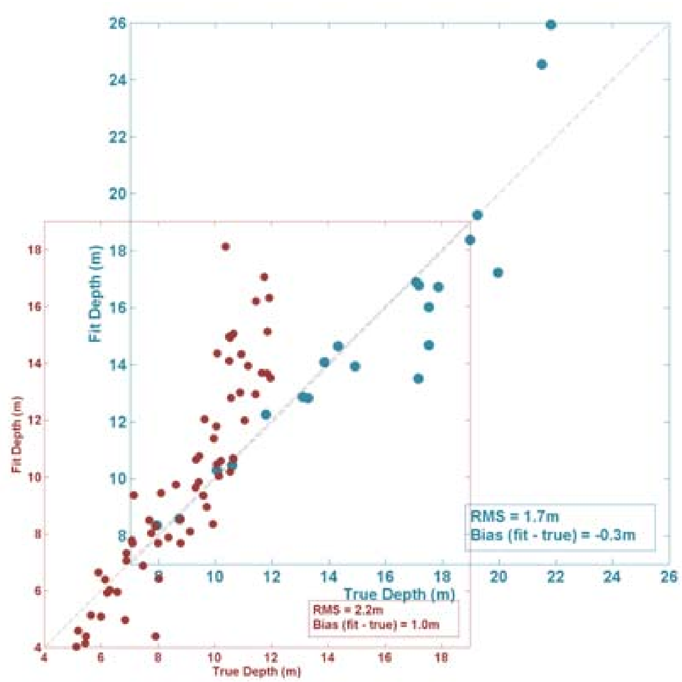

Figure 17. Cape Henry retrievals at 336 m and 672 m tiles. The depth retrievals from the 336 m (red) and 672 m (blue) and all points where there was a successful retrieval are shown. Not that the bias observed in the 336 m tiles beyond 10 m is not observed in the 672 m tiles.

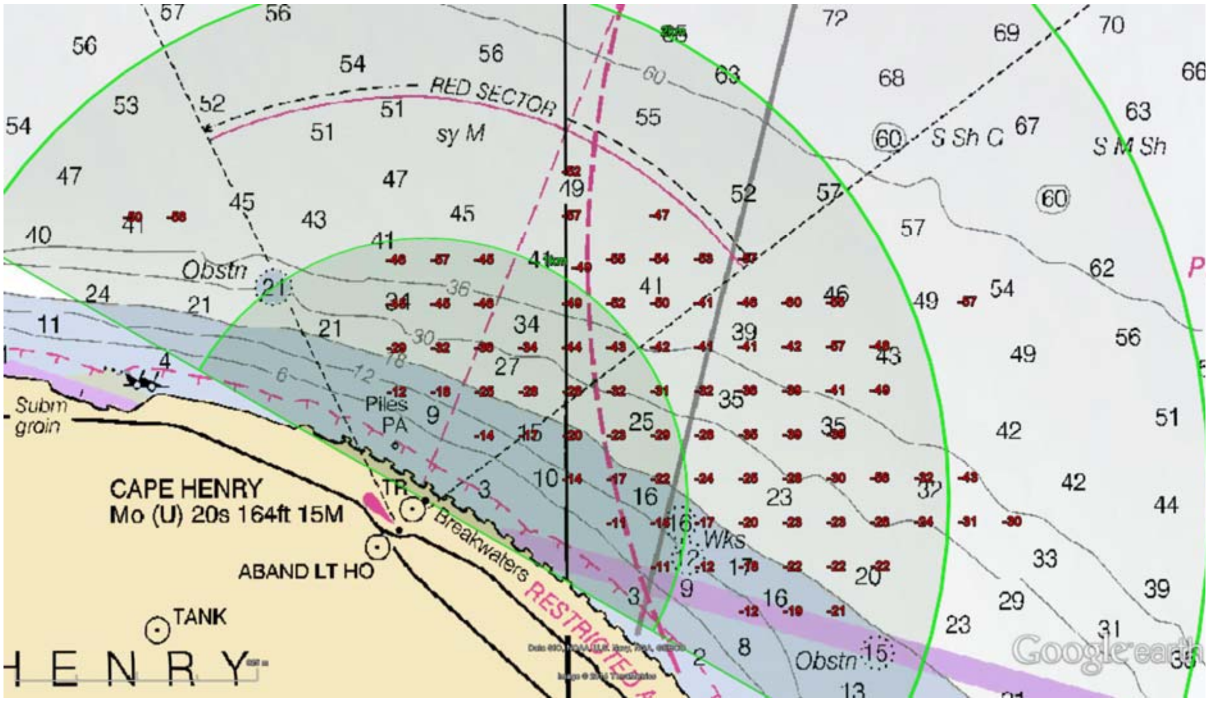

Figure 18. Cape Henry Radar Bathymetry. This is NOAA Chart #12254 with the radar bathymetry overlaid. The red numbers are the bathymetric radar retrievals from the 336m x 336m tiles with 50% overlap. The green rings indicate ranges of 1 km, 2 km and 3 km

5) Discussion

We successfully demonstrated bathymetric radar retrievals with an existing algorithm showing an accuracy of approximately 1 m or better over depths ranging from 4 to 20 meters.

a) Feasibility and Technology Risk

To explore feasibility of operational bathymetric radar, we first benchmark the results against the performance metrics. Table 3 presents a table of those metrics against the results of this study.

We demonstrated the temporal resolution that would allow for observation tidal variability in water depth. We also successfully demonstrated the performance metric depth ranges

We did not achieve 3000 m in range. One problem was that at the Cape Henry location the depths exceeded 20m at ranges beyond 2000m. This site limited the ability to demonstrate absolute range limits. The bias was within the performance metric but there is some RMS variability. However, to improve the range and accuracy we should leverage the full capability of the radar hardware and optimize the pre-processing.

The radar hardware allows for range dependent gain control. This allows the user to increase the gain as a function of range and thus compensate for the weaker returns at far range and optimize the dynamic range of the analog to digital processor. This will give better SNR at far range. The software that interfaces with the radar could be better optimized for this gain control and perhaps dynamically adjust the parameters based on the wave conditions.

The pre-processing can be refined to also increase the SNR and this will improve both range and accuracy. First, there is some image to image jitter. This jitter effectively smears out wave variance and dispersion information in the 3-D PSD. Removal of the jitter is straight forward and will be done on the next phase. Second, there are some boats that transit through the radar's field of view. While the boats are small, they do add noise to the 3-D PSD. A simple boat tracker algorithm should be implemented to remove their signatures prior to depth retrieval processing.

The three major sources of technology risk are operational implementation of a next generation algorithm, natural variability in wind and wave conditions and implementation of a meaningful error metric.

A next generation algorithm is the path towards improved accuracy, but more importantly, improved spatial resolution. However, there is some technology risk with this approach. Further work is needed to provide guidance for the implementation of universal computational geometries and optimization of parameters. This can be achieved with further study of real radar data and ground truth comparisons.

The natural variability in wave signature strength is a source of risk. Waves long enough to shoal and high enough to be detected must be present for depth retrievals. In addition, there must be some wind to generate the surface roughness (clutter) in order to detect the waves with the radar. A long term collection and analysis is required to fully understand how changes in winds and waves impact the system performance. A one-month continuous data collection will be proposed for Phase II. This will allow us to better understand how these environmental parameters modulate system performance and allow for prediction of system performance over a range of conditions.

We have not yet touched on the implementation of error metrics. An operational system must be able to provide a self consistent metric of error with each depth retrieval. The accuracy of each depth retrieval is expected to vary with wind and wave conditions. So it is important to implement error metrics. We do have error metric~~s~~ with the 3-D PSD algorithm based on SNR and goodness-of-fit metrics that were developed for airborne passive imagery. A next generation algorithm will also provide an error metric based on consistency in the iterative processing. Either approach can readily be implemented with the radar data. However, we must first have the proposed long-term retrievals in order to validate the metrics.

Table 3. Feasibility Metrics.

	Metric	3-D PSD Demonstrated	Path Forward
Range	3000 m	2000 m	• Leverage full capability of radar hardware • Refine pre-processing
Spatial Resolution	100 m	336 m for < 10m 672 for 10-20m	• Next generation algorithm
Temporal Resolution	30-60 minutes	30 minutes	*achieved*
Accuracy	25 cm	Bias: <0.3m RMS: <1 m	• Next generation algorithm
Depth Range	3m (outside surf zone) to 20 m	4 m (surf) to 20 m	*achieved*

b) Considerations for Operational Implementation

There are implementation considerations for an operational system. These include practical guidance to radar site selection and system implementation.

The implementation should first leverage existing radar infrastructure. There are many sites, including Cape Henry, that already have x-band radars suitable for bathymetry. However, bathymetric radar will be limited to locations where there are longer ocean waves present. It clearly will not work in a protected harbor, estuary or river. It will only work where ocean swell is present at least some of the time. Historical wind and wave data, along with the range of expected depths, should be considered as part of the site selection process. The radar height should also be a consideration as this impacts range.

The computational requirements are relatively modest and commercial off the shelf desktop computers can readily provide processing. Cloud based computing may provide an implementation path. This would leverage existing data networks to carry the radar data to a remote data assembly center for processing, dissemination and processing. This approach reduces the maintenance cost because software and computer installation and updates would not require site visits. It also assures data quality assurance and control to be consistently applied across location.

This study addresses a shore based bathymetric radar system. However, all the lessons learned are directly applicable to a ship based radar system. In this application, a ship would use its x-band radar to survey the surrounding bathymetry in real-time. This look-ahead capability would improve navigation safety, especially in areas with poor bathymetric coverage or following a dynamic sediment transport even such as a hurricane. This could also be used to rapidly survey a near shore location remotely from a stand-off distance.

Data streams from an operational radar system would provide capabilities beyond just bathymetry. Operational radars, such as those located at the Pilot's Tower at Cape Henry, are used for monitoring vessel traffic. However, appropriate algorithms may also provide real-time surface currents, wave heights, tide stage, oil spill tracking and continuous monitoring for potential hazards to navigation. While these applications are beyond the scope of this effort, all the data collection and data pre-processing conducted under this study would be directly relevant to these applications as well. The cloud-based processing would be an efficient framework for adding these new capabilities in the future.

Finally, NOAA will need to develop specific requirements and operational guidelines so that the bathymetric systems are consistently applied. This would be similar to standards set for acoustic and LiDAR bathymetric surveys set by the IHO. This will allow the end users to develop confidence in the technology.

6) References

Aragh, S. and O. Nwogu (2008). "Variational Assimilation of Synthetic Radar Data into a Pseudo-spectral Wave Model." J. Coastal Res. - Special Issue 52 - Surface Water Modeling **52**: 235-244.

Bell, Paul S: Shallow water bathymetry derived from an analysis of X-band marine radar images of waves, Coastal Engineering, Volume 37, Issues 3–4, August 1999, Pages 513-527, ISSN 0378-3839,

Blondel-Couprie, E. and P. Naaijen (2012), Deterministic prediction of ocean waves based on X-band radar measurements, 13th Journees de l'Hydrodynamique, Lab.d'Hydrauliques Saint-Venant Ile des Impressionistes, Chatou, France

Catalan, P. A. and M. C. Haller (2008), "Remote sensing of breaking wave phase speeds with application to non-linear depth inversions." Coastal Engng. 55(1): 93-111.

Dalrymple, R.A., A.B. Kennedy, J.T. Kirby and Q. Chen (1998), Determining depth from remotely sensed images, 26th Intl. Conf. Coastal Engng. (ASCE), Copenhagen

Dierssen, H. M., and A. E. Theberge. " Bathymetry: Assessing Methods." Encyclopedia of Natural Resources. In press.

Dugan, J.P., C.C. Piotrowski and J.Z. Williams (2001), Water depth and current retrievals from airborne optical measurements of surface gravity wave dispersion, J. Geophys. Res.-Oceans, 106, C8, 16903-16915

Dugan, J.P., S.P. Anderson, C.C. Piotrowski and S. Zuckerman (2013), Airborne infrared remote sensing of riverine currents, IEEE Trans Geosci and Rem Sens 2013, 52, 9.

Frasier, S. and R. McIntosh (1996), Nonlinearities and reverse travelling energy observed in wavenumber-frequency spectra of X-band ocean backscatter, IGARSS '96, Lincoln, Nebraska

Grilli, S. T. (1998), Depth inversion in shallow water based on nonlinear properties of shoaling periodic waves, J. Coastal Engng. 35(3): 185-209

Holman, R., N. Plant, T. Holland (2013), cBathy: A robust algorithm for estimating nearshore bathymetry, J. Geophys. Res. Oceans, 118, 2595–2609, doi:10.1002/jgrc.20199.

Ludeno, G.; Flampouris, S.; Lugni, C.; Soldovieri, F.; Serafino, F., "A Novel Approach Based on Marine Radar Data Analysis for High-Resolution Bathymetry Map Generation," *Geoscience and Remote Sensing Letters, IEEE* , vol.11, no.1, pp.234,238, Jan. 2014

Piotrowski, C.C. and J.P. Dugan (2002), Accuracy of bathymetry and current retrievals from airborne optical time series imaging of shoaling waves, IEEE Trans. Geoscience and Remote Sensing, 40, 12, ~~2002,~~ 2606-2618

Plant, N.G., K.T. Holland and M.C. Haller (2008), Ocean Wavenumber Estimation From Wave-Resolving Time Series Imagery, IEEE Trans. Geoscience and Remote Sensing 46(9): 2644-2658.

Plant, W.J. and G. Farquharson (2012), Origins of features in wave number-frequency spectra of space-time images of the ocean, J. Geophys. Res. 117(C06): C06015.

Seiwell, H.R. (1947), Military oceanography in World War II, The Military Engineer, 39 (259), 202-210

Senet, C.M., J. Seemann, S. Flampouris and F. Ziemer (2008), Determination of bathymetric and current maps by the method DISC based on the analysis of nautical X-band radar image sequences of the sea surface (November 2007), IEEE Trans. Geoscience and Remote Sensing 46(8): 2267-2279.

Smith, R. A. (1996). "An operator expansion formalism for nonlinear surface waves over variable depth." J. Fluid Mech. **363**: 333-347

Trizna, D.B. (2001), Errors in bathymetric retrievals using linear dispersion in 3-D FFT analysis of marine radar ocean wave imagery, IEEE Trans. Geoscience and Remote Sensing 39(11): 2465-2469.

Trizna, D. (2010), Coherent marine radar measurements of properties of ocean waves and currents, IGARSS 2010, Honolulu: 4737-4740.

A. van Dongeren, N. Plant, A. Cohen, D. Roelvink, M.C. Haller, and P. Catalán, Beach Wizard (2008), Nearshore bathymetry estimation through assimilation of model computations and remote observations, Coastal Engng., 55, 1016-1027

Young, I. R., W. Rosenthal, and F. Ziemer (1985), A three-dimensional analysis of marine radar images for the determination of ocean wave directionality and surface currents, J. Geophys. Res., 90(C1), 1049-1059

West, B. J., K.A. Brueckner, D.M. Milder R.L. Milton (1987), A new numerical method for surface hydrodynamics, J. Geophysical Research - Oceans 92(C11): 11803-11824

Williams, W.W. (1947), The determination of gradients on enemy-held beaches, The Geographic J., 109, 1/3, 76-90

Xiao, W., Y. Liu and D. Yue (2011), Nonlinear nearshore wave environment for ship motion, 11th Intl Conf on Fast Sea Transportation (FAST 2011), ASNE, Honolulu